Università degli Studi di Padova

DIPARTIMENTO DI MATEMATICA “TULLIO LEVI-CIVITA”

Corso di Laurea Triennale in Matematica

Mathematical models for human mobility patterns: gravity model versus radiation model

Relatore:
Prof. Marco Formentin

Laureando: Elia Tiso
Matricola: 1217646

Anno Accademico 2022/2023

21 luglio 2023

Contents

Introduction: Where is George?

This dissertation will analyse the problem of searching for a mathematical foundation and explanation behind human mobility patterns. This search is not driven by a purely theoretical and abstract desire for knowledge but has strong tangible applications, the following quotation captures this aspect:

> *The dynamic spatial redistribution of individuals is a key driving force of various spatiotemporal phenomena on geographical scales* [*1*].

Such phenomena have always been of great interest; from international trade to the spread of diseases, from traffic flows to the propagation of information, the knowledge of human travel dynamics and its statistical properties have a crucial role. Thus, the modelisation of human mobility patterns aims to determine some underlying structures and dynamics of human behaviour.

Being able to make predictions is useful, if not essential, to many fields of science, with logistics as a primary example, however, this problem is particularly challenging due to human behaviour's inherent complexity. Many factors, including social interactions, primary needs and geomorphological characteristics influence humans and their choices. Additionally, human behaviour can be context-dependent, making it difficult to capture with simple mathematical models.

Since humans mobility is governed by complex environmental, sociological, technological, and urban factors, we shall define what data should be used to build such a model and how to collect them: an idea would be to utilise data on the circulation of banknotes through an online bill tracking system like *www.whereisgeorge.com* and to infer the statistical properties of human dispersal with high spatiotemporal precision.

Hank Eskin, a database consultant, founded the website *www.whereisgeorge.com* in 1998. This website gathers information from users to follow a bill (e.g. local ZIP code of the finding site and serial number of the bill) reporting the interval between sightings and the distance traveled. Initially, some rubber stamps were produced to encourage the tracking procedure, but they were discontinued due to falling under the offence of advertisement on U.S. currency. In response, Eskin enabled a point system which stimulated bill entering and the search for an already registered bill, thus creating an interesting database tracking every bill's positions at different times.

Figure 1 : *Here are some examples of marked banknotes.*

Even though this site exists for fun and because it had not been done yet [2], it has become a perfect database for the study of human mobility patterns.

> *The purpose of "Where is George?" is to track the natural and geographic circulation of money [2].*

If we reasonably assume that dollar bills are generally carried by a person, it becomes a way to track human mobility. If we note that they are also exchanged between people, it also offers an intuitive parallelism with the spread of diseases and the propagation of information. Such a simple and fun project has become an ever-growing database that Brockmann *et al.* analysed in the seminal work [1].

Brockmann's analysis showed that the dispersal of banknotes (hence the human travel pattern) can be described by a continuous random walk process incorporating scale-free jumps and long waiting times between displacements. This result was the first empirical evidence for such an ambivalent process in nature and, consequently, a starting point for the development of a novel class of models accounting for the universal features of this problem quantitatively.

We will hereafter illustrate two of the most appreciated mathematical model to describe these patterns, highlighting their strengths and weaknesses. In particular, we shall investigate the problem of commuters between two locations.

- in Chapter 1, we shall present the Gravity Model;

  Starting from an intuitive idea, this model is the most historical one and is still used and studied to this day due to its simplicity. However, there often are inconsistencies with its results and its validity is all but verified by the collected data. In particular, an example comparing two predictions in Utah and Alabama (U.S.) will play a central role. While the variables for the Gravity Model are very similar hence producing a similar prediction on the number of commuters between the pair of chosen locations, the U.S. Census registered a substantial difference (more on Section 1.1.3).

- in Chapter 2, we shall present the Radiation Model;

  This model tried to solve some of the biggest problems of the previous one and succeeded, even becoming parameter-free. While the Gravity Model was inspired by Newton's gravitational law, the Radiation Model was created in analogy with the absorption-emission processes of particles [3]. Although we cannot consider this search concluded, it has surely heightened our comprehension of the mathematical structure behind human mobility patterns.

- in Chapter 3, we shall present some numerical results comparing these two models in a fictional case and the Utah-Alabama case, which will have accompanied the reader throughout this dissertation.

Chapter 1

Gravity Model

The Gravity Model is one of the most important models used in location analysis to describe mobility patterns. Introduced in 1946, but with roots that go back to the eighteenth century, this model is built in analogy with Newton's law of the gravitational force. This law states that the gravitational force F_{ij} between two masses m_i and m_j separated by a distance d_{ij} is given by

$$F_{ij} = \gamma \frac{m_i m_j}{d_{ij}^2}$$

where γ is a constant.

Since our analysis is concerned with the spatial locations of activities, such as the journey from home to work, we shall hereafter consider T_{ij} as the number of individuals that move per unit of time, m_i the population of the origin location i, m_j the population of the destination location j and d_{ij} as the travel distance between locations i and j per unit of time. We define a first form of the Gravity Model through the law

$$T_{ij} = k \frac{m_i m_j}{d_{ij}^2} \tag{1.1}$$

where k is a constant.

This law could be generalised by noting that there is no reason to think that T_{ij} is inversely proportional to the square of the distance d_{ij}, but only that there is a relationship between T_{ij} and c_{ij}, a generalised cost of travelling from i to j. A further generalisation would be to consider that T_{ij} is proportional to some power of m_i and m_j, and decays with the cost c_{ij}.

Definition 1. Given the following

- i, j locations in *Region A*;
- T_{ij} the number of individuals that move per unit of time between i and j;
- m_i the population of the origin location i;
- m_j the population of the destination location j.

Then, the Gravity Model [GM] is defined by the law

$$T_{ij} = \frac{m_i^{\alpha} m_j^{\beta}}{f(c_{ij})} \tag{1.2}$$

where α, β are adjustable exponents, c_{ij} is the generalised cost of travelling from i to j and $f(c_{ij})$ is the deterrence function chosen to fit the empirical data.

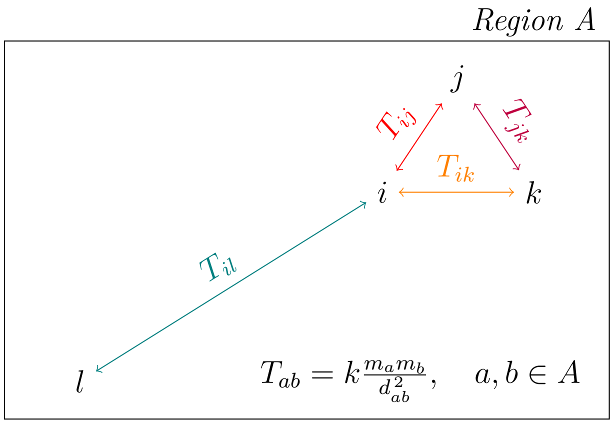

Figure 1.1 : *In this Figure, we present an intuitive visualisation of the amount* T_{ij} *using the law defined in Equation* (1.1)*. Inside the Region A are the locations* i, j, k *and* l*. Assuming*

$$d_{il} > d_{ij} \sim d_{ik} \sim d_{jk} \quad \textit{where} \quad d_{ab} = |a - b| \quad \textit{for} \quad a, b \in A,$$

we can deduce that, if $m_i = m_j = m_k = m_l$*, then*

$$T_{il} < T_{ij} \sim T_{ik} \sim T_{jk}.$$

Whereas, if $m_i = m_j = m_k << m_l$*, it may not be the case. These obvious notes emphasise how few variables can totally alter the result, much less considering the form presented in Equation* (1.2)*.*

1.1 Some problems of the Gravity Model

Despite its widespread use, this law has some notable limitations that left researchers doubtful of its actual validity. Let us note that the simplicity and intuitivity of this model still attract today, allowing its use in some areas of logistics.

The above-mentioned limitations will be hereunder listed and analysed:

(i) lacking a rigorous derivation of Equation (1.2);

Although many studies have proved the effectiveness of the GM [4], it has yet to be rigorously deduced. Looking at the particular case of the gravity law with $\alpha = \beta = 1$, it is possible to use the entropy maximising method to obtain a derivation. However, it has to be noted that this result does not resolve the substantial problem, which therefore remains, but only helps in giving a clearer vision of this law.

This result will be presented in Section 1.1.1.

(ii) lacking theoretical guidance, the deterrence functions used are of various forms and have many parameters;

The pursuit for a universally valid function has lasted decades and while many results confirm the GM's validity, they still fail to provide its theoretical derivation. With this in mind, it has been proposed that the empirical success of the GM, although not matched with its theoretical counterpart yet, shall be accepted as a fact of life [4].

This result will be presented in Section 1.1.2.

(iii) this model is unable to predict mobility in regions where systematic traffic data are lacking;

The ability to use this model with limited data is crucial, thus this barrier remains quite visible. This may be one of the most critical problems of this model since it would difficult to calibrate the law without adding many parameters, which is something that would divert us from a universal description of human mobility.

(iv) it has systematic predictive discrepancies;

An example of the predictiveness unreliability will be presented subsequently: two pairs of U.S. counties with similar origin and destination populations and comparable distance will highlight how, although the GM predicts that they should have a similar flux of people, their fluxes of people differ of an order of magnitude.

This result will be presented in Section 1.1.3.

(v) Equation (1.2) predicts that the number of commuters increases without limit as we increase the destination population m_j, yet it cannot exceed the origin population m_i, highlighting an analytical inconsistency;

It will be later shown in Section 1.1.1 how to overcome this problem by adding certain constraints.

(vi) being deterministic, it cannot account for fluctuations in the number of travellers between the two populations, while this trait would be of great interest.

1.1.1 Derivation through the entropy maximisation

It is possible to consider a particular case of the gravity law, with $\alpha = \beta = 1$, and use the entropy maximisation [5][6] to derive Equation (1.2). However, it still fails to offer the functional form of $f(c_{ij})$ making this work only partially satisfying.

Remark 1. The aforementioned introduction is slightly improper: we shall use the entropy maximisation method on a probability distribution. It will be now used $\{T_{ij}\}$ to define the distribution of trips.

Remark 2. In order to better illustrate this example, the following notation will be helpful. Let the number of trip origins in i be noted as O_i and the number of trip destinations in j be noted as D_j, both are proportional to T_{ij}, which will now represent the total number of trips from i to j.

Remark 3. As previously stated in Item (v), the analytical inconsistency of the number of commuters needs to be addressed. To correct such behaviour, let us add two constraints:

$$\sum_j T_{ij} = O_i, \tag{C.1}$$

$$\sum_i T_{ij} = D_j. \tag{C.2}$$

These can be satisfied by introducing a set of A_i and B_j sometimes called balancing factors. Still, these constraints cannot solve the substantial problem of Equation (1.2).

Definition 2. In light of the above notations and remarks, the gravity law with $\alpha = \beta = 1$ will be henceforth written as

$$T_{ij} = A_i B_j O_i D_j f(c_{ij}) \tag{1.3}$$

where $f(c_{ij})$ is some decreasing function cost, and

$$A_i = \frac{1}{\sum_j B_j D_j f(c_{ij})},$$
$$B_j = \frac{1}{\sum_i A_i O_i f(c_{ij})}$$

satisfy Equations (C.1) to (C.2). It will be also assumed another constraint

$$\sum_{i,j} T_{ij} c_{ij} = C \tag{C.3}$$

which implies that the total amount spent on trips in the region from which i and j are located at a certain point in time is a fixed amount C.

The crucial assumption of the entropy maximising method is now stated.

Assumption. The probability $\mathbf{P}$ of the distribution $\{T_{ij}\}$ occurring is proportional to the number of states of the system which satisfy the constraints. Thus, if $w(T_{ij})$ is the number of ways in which individuals can be arranged to produce the overall distribution $\{T_{ij}\}$, then it can be written as

$$\mathbf{P}(\{T_{ij}\}) \propto \sum w(T_{ij})$$

where the summation is restricted to those T_{ij} that satisfy the constraints Equations (C.1) to (C.3).

Supposing

$$T = \sum_i O_i = \sum_j D_j \tag{1.4}$$

is the total number of trips, the number of distinct arrangements of individuals which give rise to $\{T_{ij}\}$ is

$$\begin{aligned} w(T_{ij}) &= \binom{T}{T_{11}} \cdot \binom{T - T_{11}}{T_{12}} \cdot \ldots \\ &= \frac{T!}{T_{11}!\cancel{(T - T_{11})!}} \cdot \frac{\cancel{(T - T_{11})!}}{T_{12}!\cancel{(T - T_{11} - T_{12})!}} \cdot \ldots \\ &= \frac{T!}{\prod_{i,j} T_{ij}!} \end{aligned}$$

and the total number of possible states is then

$$W = \sum w(T_{ij})$$

where the summation is restricted to those T_{ij} that satisfy the constraints Equations (C.1) to (C.3).

All of the necessary ingredients for proving the following have now been given.

Proposition 1. *It is possible to derive*

$$T_{ij} = A_i B_j O_i D_j f(c_{ij})$$

through the entropy maximisation method. In particular, it will be obtained $f(c_{ij}) = \exp[-\beta c_{ij}]$ *where* β *is a Lagrangian multiplier.*

Proof. The study of

$$W = \sum w(T_{ij})$$

shows that the maximum values of $w(T_{ij})$ dominate the other values of the sum to such an extent that the distribution $\{\overline{T}_{ij}\}$ such that $\max_{T_{ij}} w(T_{ij}) = w(\overline{T}_{ij})$ is predominantly the most probable distribution.

Hence this method is a probability-maximising method.

The maximum will now be obtained through the maximisation of the function $w(T_{ij})$ subject to the constraints

$$\begin{aligned} h_i &\stackrel{\text{def}}{=} \sum_j T_{ij} - O_i, \\ k_j &\stackrel{\text{def}}{=} \sum_i T_{ij} - D_j, \\ l &\stackrel{\text{def}}{=} \sum_{i,j} T_{ij} c_{ij} - C. \end{aligned}$$

We shall use the method of Lagrange multipliers to find it.

Theorem 1 (Lagrange multipliers Theorem)**.** *Let* $A \subset \mathbb{R}^n$ *be an open set,* $f \in C^1(A)$ *and* $M \in A$ *a differentiable manifold of dimension* $d \in \{1, \ldots, n-1\}$ *such that*

$$M \stackrel{\text{def}}{=} \{h = 0\} \quad \textit{where} \quad h \in C^1(A; \mathbb{R}^{n-d}).$$

If f *attains a local extremum at* $\bar{x} \in A \cap M$*, then there exist* $\lambda_1, \ldots, \lambda_{n-1} \in \mathbb{R}$*, called Lagrangian multipliers, such that*

$$\nabla f(\bar{x}) = \sum_{j=1}^{n-d} \lambda_j \nabla h_j(\bar{x}).$$

Since it is more convenient to work with $\log w$ rather than w and, therefore, be able to use Stirling's approximation

$$\log N! = N \log N - N \tag{1.5}$$

to estimate the factorial terms, let f be $\log w$ and let the constraints h_i, k_j, l define M. Let us define a new function Q as

$$\begin{aligned} Q &\stackrel{\text{def}}{=\!=} f - \sum_i \lambda_i^{(1)} h_i - \sum_j \lambda_j^{(1)} k_j - \beta l \\ &= \log w + \sum_i \lambda_i^{(1)} \left(O_i - \sum_j T_{ij} \right) + \sum_j \lambda_j^{(2)} \left(D_j - \sum_i T_{ij} \right) + \beta \left(C - \sum_{i,j} T_{ij} c_{ij} \right) \end{aligned}$$

where $\lambda_i^{(1)}$, $\lambda_j^{(2)}$ and β are Lagrangian multipliers.

The values that maximise Q, which as previously stated constitute the most probable distribution of trips, are the solutions of

$$\frac{\partial}{\partial T_{ij}} Q = 0 \tag{1.6}$$

and the constraints Equations (C.1) to (C.3). Using Equation (1.5), note that

$$\frac{\partial}{\partial N} \log N! = \frac{\partial}{\partial N} N \log N - \frac{\partial}{\partial N} N = \log N$$

thus

$$\begin{aligned} \frac{\partial}{\partial T_{ij}} \log w(T_{ij}) = \frac{\partial}{\partial T_{ij}} \log \frac{T!}{\prod_{i,j} T_{ij}!} &= \cancel{\frac{\partial}{\partial T_{ij}} \log T!} - \frac{\partial}{\partial T_{ij}} \log \prod_{i,j} T_{ij}! \\ &= - \frac{\partial}{\partial T_{ij}} \sum_{i,j} \log T_{ij}! = - \log T_{ij} \end{aligned}$$

which gives

$$\frac{\partial}{\partial T_{ij}} Q = - \log T_{ij} - \lambda_i^{(1)} - \lambda_j^{(2)} - \beta c_{ij}$$

that, in order to obtain Equation (1.6), implies that

$$T_{ij} = \exp \left[-\lambda_i^{(1)} - \lambda_j^{(2)} - \beta c_{ij} \right]. \tag{1.7}$$

Substituting Equation (1.7) in Equation (C.1), it is possible to obtain $\lambda_i^{(1)}$:

$$\begin{aligned} \sum_j T_{ij} &= O_i, \\ \sum_j \exp \left[-\lambda_i^{(1)} \right] \exp \left[-\lambda_j^{(2)} - \beta c_{ij} \right] &= O_i, \\ \exp \left[-\lambda_i^{(1)} \right] \sum_j \exp \left[-\lambda_j^{(2)} - \beta c_{ij} \right] &= O_i, \end{aligned}$$

hence

$$\exp \left[-\lambda_i^{(1)} \right] = \frac{O_i}{\sum_j \exp \left[-\lambda_j^{(2)} - \beta c_{ij} \right]}. \tag{1.8}$$

Analogously, it is possible to obtain $\lambda_j^{(2)}$ from Equation (C.2):

$$\exp \left[-\lambda_j^{(2)} \right] = \frac{D_j}{\sum_i \exp \left[-\lambda_i^{(1)} - \beta c_{ij} \right]}. \tag{1.9}$$

The same result can be expressed in a more familiar form by writing

$$
\begin{aligned}
A_i &= \frac{\exp\left[-\lambda_i^{(1)}\right]}{O_i}, \\
B_j &= \frac{\exp\left[-\lambda_j^{(2)}\right]}{D_j}
\end{aligned}
$$

and then

$$T_{ij} = A_i B_j O_i D_j \exp\left[-\beta c_{ij}\right]$$

where, using Equations (1.8) to (1.9),

$$
\begin{aligned}
A_i &= \frac{1}{\sum_j B_j D_j \exp\left[-\beta c_{ij}\right]}, \\
B_j &= \frac{1}{\sum_i A_i O_i \exp\left[-\beta c_{ij}\right]}.
\end{aligned}
$$

It is yet to be explained why is the entropy involved.

Definition 3. Given a number of system states with a significant probability of being occupied and letting p_i be the probability that the system is in i-th state, the entropy is defined as

$$S = -k_B \sum_i p_i \log p_i$$

where k_B is the Boltzmann constant.

If we define

$$p_{ij} \stackrel{\text{def}}{=\!=} \frac{T_{ij}}{T} \quad \text{and} \quad H = -\sum_{i,j} p_{ij} \log p_{ij}$$

it is easy to check that maximising H under the constraints Equations (C.1) to (C.3) gives the same answer as the previous approach.

Thus, such a method is called entropy maximisation. ■

1.1.2 The choice of the deterrence function

The choice of the deterrence function is an important step that defines the gravity model. It is often proposed an exponential function $f(d_{ij}) = \exp\left[\gamma d_{ij}\right]$, where d_{ij} is the distance between the origin and destination location and γ an appropriate parameter.

As an example, in the field of multi-scale mobility networks, Table 1.1 presents values for the parameters α, β, γ of the gravity law

$$T_{ij} = C \frac{m_i^{\alpha} m_j^{\beta}}{\exp\left[\gamma d_{ij}\right]} \tag{1.10}$$

where C is a constant and the other variables assume the roles previously stated, such as m_i for the population of the origin location i, m_j for the population of the destination location j and d_{ij} for the travel distance between i and j.

d(km)	Parameter	Estimate	Standard Error
≤ 300	α	0.46	0.01
	β	0.64	0.01
	γ	0.0122	0.0002
> 300	α	0.35	0.06
	β	0.37	0.06

Table 1.1 : *In this Table, we present the exponents of the gravity law given by Equation* (1.10) *as obtained by applying a multivariate analysis to global commuting data* [7].

While probing for the appropriate exponents' tuning, the existence of two different regimes in T_{ij} emerged [7]: we observe a flattening of the commuter flows at around 300 km. Considering this fact, it seemed appropriate to subdivide this inquiry into two and tune the parameters accordingly. For the foregoing reasons, if $d_{ij} > 300$ km, the value of $f(d_{ij})$ is definitely constant and thus it is possible to solely search for the parameters α and β.

However, this formulation of the deterrence function is not accepted by all, and many have defined and empirically fit other forms. These attempts to theoretically derive the gravity law have nevertheless regrettably met poor success. On this note, Alan Deardorff, professor emeritus of International Economics, wrote the following

> *I suspect that just about any plausible model of trade would yield something very like the gravity equation, whose empirical success is therefore not evidence of anything, but just a fact of life* [4].

1.1.3 Real-life application: Utah and Alabama

In this section are shown two pairs of U.S. counties with similar origin and destination populations and comparable distances that exemplify how, despite the gravity model estimating a similar flux of people for the two for them, the U.S. Census has collected data that differ by an order of magnitude.

For our purpose, it suffices the following version of the gravity law

$$T_{ij} = \frac{m_i^{\alpha} m_j^{\beta}}{d_{ij}^{\gamma}}. \tag{1.11}$$

The counties taken into consideration are Davis County and Washington County (Utah) and Madison County and Houston County (Alabama) and the travel starts from the first to the second one of each set.

Fitting the gravity model to U.S. workflow data, 3109 counties in 49 continental U.S. states have been used, yielding 161,710 pairs of counties with a non-zero flow of workers [8]. To better illustrate the gravity model behaviour, the parameters are fitted separately for distances above and below 119 km (similarly to what has been observed in Section 1.1.2). Up to this threshold, a rapid decline in the movements to the destination j in respect of the distance d_{ij} has been observed which means that the value γ makes d_{ij} highly relevant. On the other hand, beyond that, a small flux of movements is nearly independent of distance, meaning that the value γ is close to zero.

	Utah	Alabama
m_i	240,000	280,000
m_j	90,000	89,000
d_{ij}	447	410

(a)

	$d_{ij} < 119$ km	$d_{ij} \geq 119$ km
α	0.30	0.24
β	0.64	0.14
γ	3.05	0.29

(b)

Table 1.2 : *In these Tables, we present the values used in the gravity law defined by Equation* (1.11) *and fitted to the dataset above. In Table 1.2a are the values of the population and distance for the location i and j of each set as collected by the U.S. Census 2000 [3] and in Table 1.2b the values of the parameters α, β and γ. Although Table 1.2b includes findings for both distance ranges for completeness, we shall focus on the last column.*

The U.S. Census 2000 dataset for the commuters amount between counties, i.e. the values T_{ij}, has been removed from the government site, however, by calculating the prediction using the available data from the U.S. Census 2010, compatible results are obtained.

Using the information in Table 1.2, it is possible to obtain an estimation of the flux from i to j for each set as follows

$$T_{ij}^{UT} = \frac{m_i^\alpha m_j^\beta}{d_{ij}^\gamma} = \frac{(240000)^{0.24}(90000)^{0.14}}{(447000)^{0.29}} \sim 2,22,$$
$$T_{ij}^{AL} = \frac{m_i^\alpha m_j^\beta}{d_{ij}^\gamma} = \frac{(280000)^{0.24}(89000)^{0.14}}{(410000)^{0.29}} \sim 2,36.$$

Theoretically, since the values of T_{ij}^{UT} and T_{ij}^{AL} are close, if the GM has good predictive power, we should have similar results from the dataset. However, the U.S. Census 2000 reports a flux that is an order of magnitude greater between the Utah counties:

	Utah	Alabama
m_i	240,000	280,000
m_j	90,000	89,000
d_{ij}	447	410
C	44	6
GM	2	2

Table 1.3 : *Starting from Table 1.2a, we add the flux of people from location i to location j as observed by the U.S. Census 2000 [C] and as predicted by the Gravity Model defined by Equation* (1.11) *and fitted with the parameters from Table 1.2b [GM].*

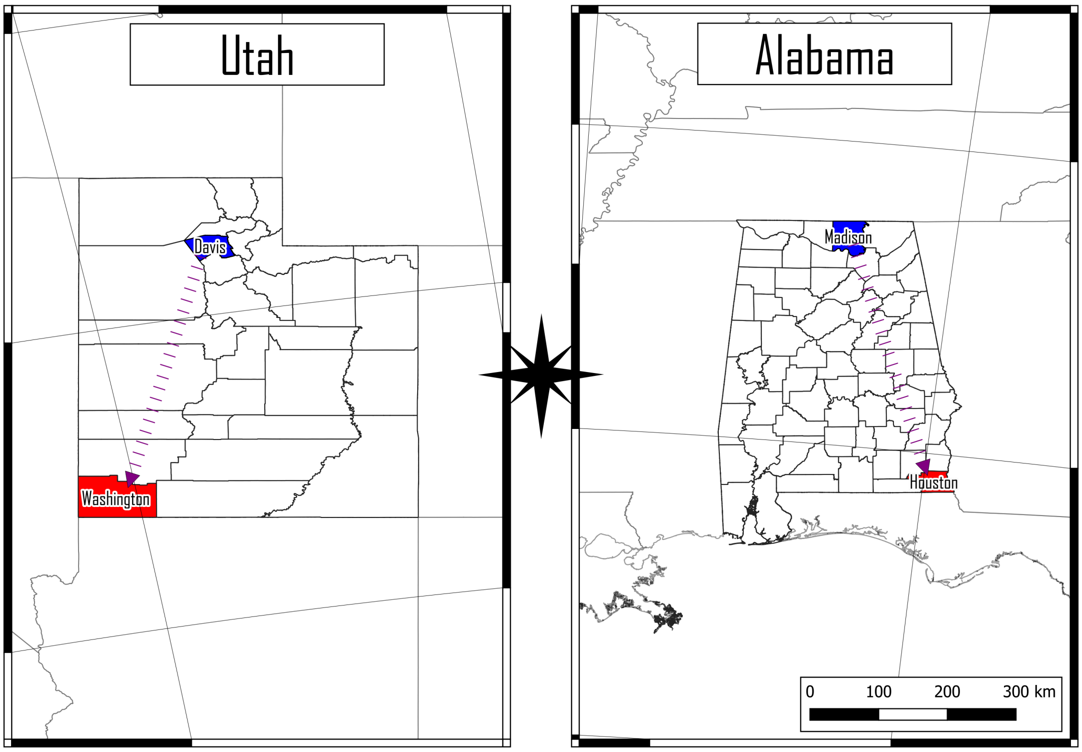

Figure 1.2 : *In this Map, we highlight the counties used as an example in this section, using the same scale to show the similar distance.*

This example will be later resumed using a different model capable of capturing better results.

Chapter 2

Radiation Model

To overcome the limitations above-analysed, many variants of the Gravity Model have been proposed but did not solve all of them. Even alternative approaches like the Intervening Opportunity Model and the Random Utility Model only partially solved these problems. They still contained, withal, context-specific tunable parameters, and their predictive power was at best comparable to the gravity law. A point in favour of these new approaches is the idea to derive a new model from first principles, thus, comprehending what actually determines the commuting of people. We shall present a new model that became a serious contender to the GM: the Radiation Model [3].

Ergo, the core of the model hereunder presented is that, while commuting is a daily process, its origin and destination are determined by a decision made over longer timescales: the job selection.

Using the natural partition of a country into counties (as in Section 1.1.3), the job selection is assumed to consist of two steps:

1. an individual seeks job offers from all counties, including theirs;

   The number of opportunities in each county is proportional to its population, n, assuming that there is one job opening for every n_{jobs} individuals. Let us capture the benefits of a potential employment opportunity from a distribution $p(z)$, where z represents a combination of working schedule, income, conditions, and the like. Every county with n population is, thus, assigned $\bar{n} = n/n_{jobs}$ employment opportunities $z_1, \ldots, z_{\bar{n}}$, hinting that larger a county's population, the more employment opportunities it offers.

2. the individual chooses the closest job to their home, whose benefits z are higher than the best offer available in their home county.

   Note that lack of commuting has priority over the benefits.

This model has three unknown parameters:

- $p(z)$ the benefit distribution;
- n_{jobs} the job density;
- T the total number of commuters (as used in Equation (1.4) in Section 1.1.1).

Our aim is to need the least amount of parameters possible. It will be later shown that the commuting fluxes T_{ij} are independent of $p(z)$ and n_{jobs}, and that T does not affect the flux distribution, making this model parameter-free. As the model can be formulated in terms of radiation and absorption processes, it will be referred to as the Radiation Model.

Definition 4. Given the following

i, j locations in *Region A*;

T_{ij} the number of individuals that move per unit of time between i and j;

m_i the population of the origin location i;

m_j the population of the destination location j;

d_{ij} the euclidean distance between i and j;

s_{ij} the total population in the circle of radius d_{ij} centred at i excluding the origin and destination locations.

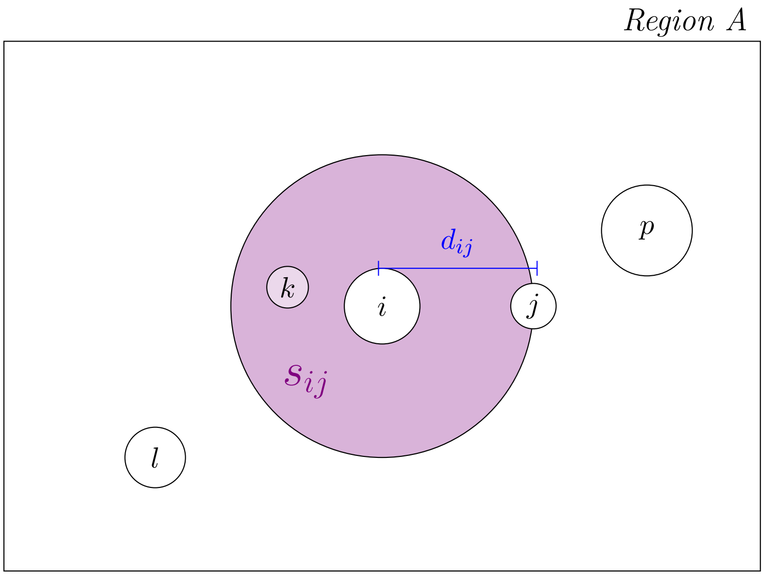

Figure 2.1 : *In this Figure, an intuitive visualisation of the amount s_{ij} is presented.*

The average flux predicted by the Radiation Model [RM] is then

$$\langle T_{ij}\rangle = T_i \frac{m_i m_j}{(m_i + s_{ij})(m_i + m_j + s_{ij})} \tag{2.1}$$

where

$$T_i = \sum_{j \neq i} T_{ij}$$

is the number of commuters with origin location i and destination location $j \neq i$.

Remark 1. The Equation (2.1) is independent of both $p(z)$ and n_{jobs}. Since T_i is proportional to the population of the origin location i,

$$T_i = m_i \left(\frac{T}{N}\right) \tag{2.2}$$

where T is the total number of commuters and N is the total population of the country.

Remark 2. Another form of these two parameters would be

$$T = \sum_i O_i = \sum_j D_j \quad \text{and} \quad N = \sum_i m_i$$

where we recall O_i being the number of trip origins in i, and D_j being the number of trip destinations in j. This formulation will not be further used, but it is effective in showing the difference between the two.

Briefly summarising the prior study, the major problems were the following

(i) lacking a rigorous derivation of Equation (1.2);

(ii) lacking theoretical guidance of the deterrence function, particularly in regard to the parameters;

(iii) the GM is unable to predict mobility in regions where systematic traffic data are lacking;

(iv) the GM has systematic predictive discrepancies;

(v) Equation (1.2) predicts that the number of commuters increases without limit as we increase the destination population m_j, yet it cannot exceed the origin population m_i, highlighting an analytical inconsistency;

(vi) being deterministic, it cannot account for fluctuations in the number of travellers between the two populations, while this trait would be of great interest.

The radiation model defined by Equation (2.1) resolves the limitations exhibited in Items (i) to (vi) and analysed throughout Section 1.1.

It has a rigorous derivation (resolving Item (i)) and no free parameters (resolving Item (ii) and Item (iii)). The problem exposed in Item (iv) is addressed by observing the population density around i: for uniform population density

$$s_{ij} \sim m_i d_{ij}^2 \quad \text{and} \quad m = m_i = m_j, \quad \forall i, j \tag{$\star$}$$

from the RM we obtain

$$\begin{aligned} T_{ij}\Big|^{RM} &= T_i \frac{m_i m_j}{(m_i + s_{ij})(m_i + m_j + s_{ij})} \xrightarrow{(\star)} T_i \frac{\cancel{m^2}}{\cancel{m}(1 + d_{ij}^2)\cancel{m}(2 + d_{ij}^2)} \\ &\xrightarrow{(2.2)} m \frac{T}{N} \frac{1}{(1 + d_{ij}^2)(2 + d_{ij}^2)} \sim \frac{m}{d_{ij}^4} \end{aligned}$$

on the other hand, using

$$f(d_{ij}) = d_{ij}^{\gamma},\ \gamma = 4,\ \alpha + \beta = 1 \tag{$\star\star$}$$

in the GM, we obtain

$$T_{ij}\Big|^{GM} = C \frac{m_i^{\alpha} m_j^{\beta}}{f(d_{ij})} \xrightarrow{(\star\star)} C \frac{m^{(\alpha+\beta)}}{d_{ij}^{\gamma}} = C \frac{m}{d_{ij}^4} \sim \frac{m}{d_{ij}^4}$$

showing that the radiation law reduces to the gravity law. This result may hint that no progress has been made by switching the approach regarding the exhibited problem, but this is true only under the assumption that the population density is uniform, which is false in most cases.

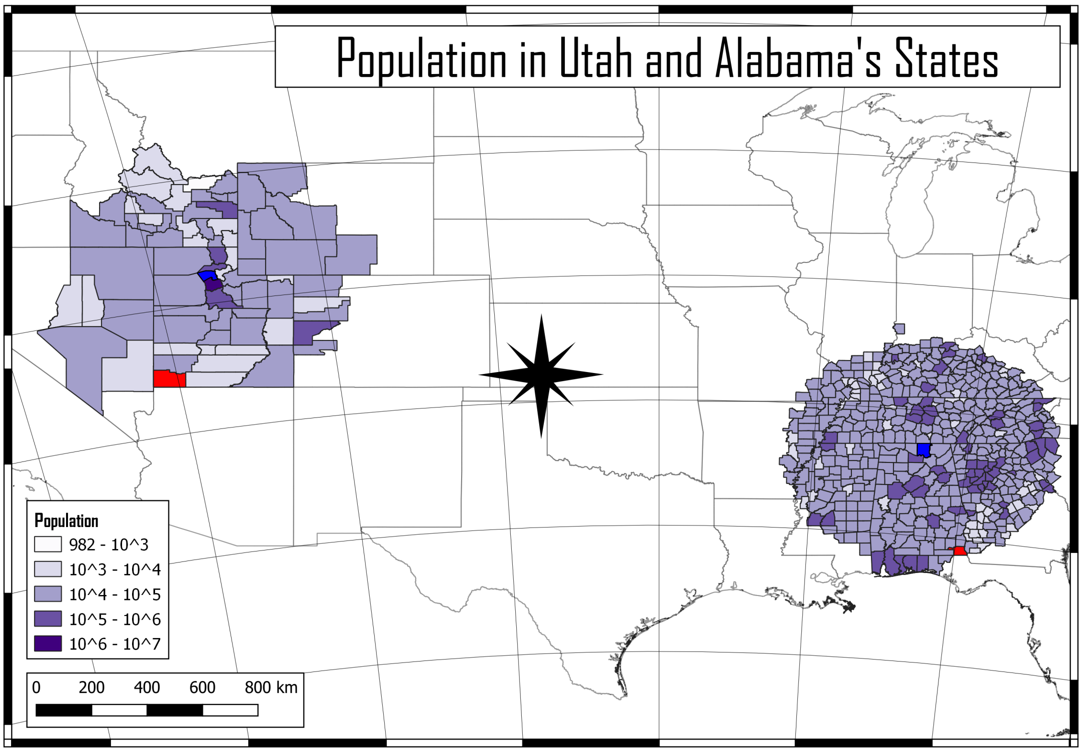

Figure 2.2 : *If we now revisit the example between the counties of Utah and Alabama and observe the value s_{ij} for $d_{ij} \sim 480$ km, it is clear that the population density around Utah is significantly lower than the U.S. average, making work opportunities within the same distance even ten times smaller in Utah than in Alabama. This implies that commuters departing from Utah have to travel farther.*

	Utah	Alabama
m_i	240,000	280,000
m_j	90,000	89,000
d_{ij}	447	410
s_{ij}	$2 \cdot 10^6$	$2 \cdot 10^7$
C	44	6
GM	2	2
RM	66	2

Table 2.1 : *Starting from the Table 1.3, the total population in the circle of radius d_{ij} centred at i excluding the origin and destination locations [s_{ij}] and the flux of people from location i to location j as predicted by the RM defined by Equation* (2.1) *[RM] are added. Let us note that the RM applied to Utah's example, using the U.S. Census 2010 dataset, gives an approximate value of 76, which is compatible with the population growth and, thus, commuters rise.*

The physical inconsistency highlighted in Item (v) is not present anymore:

$$\begin{aligned}
\lim_{m_j \to +\infty} T_{ij} &= \lim_{m_j \to +\infty} m_i \frac{T}{N} \frac{m_i m_j}{(m_i + s_{ij})(m_i + m_j + s_{ij})} \\
&= \frac{m_i^2}{(m_i + s_{ij})} \lim_{m_j \to +\infty} \frac{T}{N} \frac{m_j}{(m_i + m_j + s_{ij})} \\
&\overset{(\star)}{=} \frac{m_i^2}{(m_i + s_{ij})} \lim_{m_j \to +\infty} \cancel{\frac{N - \cancel{Q}}{N}} \frac{\cancel{m_j}}{\cancel{m_j} \left(\frac{m_i}{m_j} + 1 + \frac{s_{ij}}{m_j} \right)} \\
&= \frac{m_i^2}{(m_i + s_{ij})} \leq m_i
\end{aligned}$$

where Q is the number of non-commuters, which completes T to N, thus

$$m_j < N = T + Q. \tag{$\star$}$$

Finally, T_{ij} is now a stochastic variable predicting both the average flux between two locations (Equation (2.1)) and its variance, as it will be illustrated in the following section.

2.1 An alternative formulation of the Radiation Model

Another way to present the RM is by analogy with radiation emission and absorption processes.

Let us begin by imagining the origin location i as a source emitting an outgoing flux of identical and independent units, the process of emission-absorption is defined by two steps:

1. a number z_X^i is assigned to every particle X emitted from location i, which represents the absorption threshold for that particle; this value correspond to the maximum number obtained after m_i random extractions from a distribution $p(z)$.

   Remark 1. Since m_i is the population of the location i, particles emitted from a highly populated location have, on average, a higher *absorption threshold* than those emitted from a lower populated one.

2. the surrounding locations have a certain probability of absorbing the particle X: a number z_X^j is assigned to the surrounding location j, which represents the *absorbance* of location j for that particle.

   Remark 2. The particle is absorbed by the closest location whose absorbance exceeds its absorption threshold.

By iterating this process for all emitted particles, the fluxes across the country are obtained. The probability of an absorption-emission event occurring will be now calculated.

Definition 5. Given the following

i, j locations in *Region A*;

m_i the population of the origin location i;

m_j the population of the destination location j;

d_{ij} the euclidean distance between i and j;

s_{ij} the total population in the circle of radius d_{ij} centred at i excluding the origin and destination locations.

The probability that a particle emitted from i is absorbed in j, according to the RM, is

$$\mathbf{P}(1 \mid m_i, m_j, s_{ij}) = \int_0^{+\infty} \mathbf{P}_{m_i}(z)\mathbf{P}_{s_{ij}}(< z)\mathbf{P}_{n_j}(> z)\,\mathrm{d}z \tag{2.3}$$

where

1. $\mathbf{P}_{m_i}(z) = \mathbf{P}(\max_k x_k = z,\, k \leq m_i)$ is the probability that the maximum value extracted from the PDF $p(z)$ after m_i trails is equal to z

$$\begin{aligned}
\mathbf{P}(\max_k x_k = z,\, k \leq m_i) &= \mathbf{P}(x_k \leq z, \forall k \leq m_i - 1)\mathbf{P}(x_{\overline{k}} = z) \\
&\overset{\star}{=} m_i[\mathbf{P}(x < z)]^{m_i-1}\mathbf{P}(x = z) \\
&= m_i[p(x < z)]^{m_i-1}p(x = z) \\
&\overset{\star\star}{=} m_i[p(x < z)]^{m_i-1}\frac{\mathrm{d}}{\mathrm{d}z}p(x < z)
\end{aligned}$$

   where in $\star$ is assumed that there is only one location $\overline{k}$ at distance d_{ij} from i with the maximum absorbance value, and in $\star\star$ is used

$$\begin{aligned}
\mathbf{P}(x \leq z) &= \int_0^z \mathbf{P}(x = s)\,\mathrm{d}s \\
\frac{\mathrm{d}}{\mathrm{d}z}\mathbf{P}(x \leq z) &= \mathbf{P}(x = z)
\end{aligned}$$

2. $\mathbf{P}_{s_{ij}}(< z) = \mathbf{P}(x_k < z,\, \forall k \leq s_{ij})$ is the probability that s_{ij} numbers extracted from the $p(z)$ distribution are all lower than z

$$\mathbf{P}(x_k < z,\, \forall k \leq s_{ij}) = [\mathbf{P}(x_k < z)]^{s_{ij}} = [p(x < z)]^{s_{ij}}$$

3. $\mathbf{P}_{n_j}(> z) = \mathbf{P}(x_k > z,\, \exists k \leq m_j)$ is the probability that among m_j numbers extracted from the PDF $p(z)$ at least one is greater than z

$$\begin{aligned}
\mathbf{P}(x_k > z,\, \exists k \leq m_j) &= 1 - \mathbf{P}(x_k < z,\, \forall k \leq m_j) \\
&= 1 - [\mathbf{P}(x < z)]^{m_j} \\
&= 1 - [p(x < z)]^{m_j}
\end{aligned}$$

Therefore, Equation (2.3) represents the probability that one particle emitted from an origin location i, with population m_i, is absorbed by a destination location j, with population m_j, while not being absorbed by any closer location.

Evaluating Equation (2.3) with Items 1 to 3, we obtain

$$\begin{aligned}
\mathbf{P}(1 \mid m_i,\, m_j,\, s_{ij}) &= \int_0^{+\infty} \mathbf{P}_{m_i}(z)\mathbf{P}_{s_{ij}}(< z)\mathbf{P}_{n_j}(> z)\,\mathrm{d}z \\
&= \int_0^{+\infty} \mathbf{P}(\max_k x_k = z,\, k \le m_i)\mathbf{P}(x_k < z,\, \forall k \le s_{ij})\mathbf{P}(x_k > z,\, \exists i \le m_j)\,\mathrm{d}z \\
&= \int_0^{+\infty} m_i [p(x < z)]^{m_i - 1} \frac{\mathrm{d}p(x < z)}{\mathrm{d}z} [p(x < z)]^{s_{ij}} (1 - [p(x < z)]^{m_j})\,\mathrm{d}z \\
&= m_i \int_0^{+\infty} \left[p(x < z)^{m_i + s_{ij} - 1} - p(x < z)^{m_i + m_j + s_{ij} - 1}\right] \mathrm{d}p(x < z) \\
&\xrightarrow{t = p(x<z)} m_i \int_0^1 \left[t^{m_i + s_{ij} - 1} - t^{m_i + m_j + s_{ij} - 1}\right] \mathrm{d}t \\
&= m_i \left[\frac{1}{m_i + s_{ij}} - \frac{1}{m_i + m_j + s_{ij}}\right] \\
&= \frac{m_i m_j}{(m_i + s_{ij})(m_i + m_j + s_{ij})} \qquad (2.4)
\end{aligned}$$

Remark 3. The Equation (2.4) is independent of the distribution $p(z)$ and invariant under rescaling of the population by the same factor (n_{jobs}).

The probability for a particular sequence of absorption of the particles emitted at origin location i, $\mathbf{P}(T_{i1},\, T_{i2},\, \dots,\, T_{iL})$ into L destination locations is given by

$$\begin{aligned}
\mathbf{P}(T_{i1},\, T_{i2},\, \dots,\, T_{iL}) &= \binom{T_i}{T_{i1}} p_{i1}^{T_{i1}} \cdot \binom{T_i - T_{i1}}{T_{i2}} p_{i2}^{T_{i2}} \cdot \dots \\
&= \frac{T_i!}{T_{i1}!\cancel{(T_i - T_{i1})!}} p_{i1}^{T_{i1}} \cdot \frac{\cancel{(T_i - T_{i1})!}}{T_{i2}!\cancel{(T_i - T_{i1} - T_{i2})!}} p_{i2}^{T_{i2}} \cdot \dots \\
&= \prod_{j=1}^{L} \frac{T_i!}{T_{ij}!} p_{ij}^{T_{ij}} \quad \text{generalized with} \quad \prod_{j \ne i} \qquad (2.5)
\end{aligned}$$

where

$$\sum_{j \ne i} T_{ij} = T_i \quad \text{and} \quad p_{ij} \equiv \mathbf{P}(1 \mid m_i,\, m_j,\, s_{ij})$$

Remark 4. The distribution $\mathbf{P}(T_{i1},\, T_{i2},\, \dots,\, T_{iL})$ is normalized because

$$\sum_{j \ne i} p_{ij} = m_i \sum_{j \ne i} \left[\frac{1}{m_i + s_{ij}} - \frac{1}{m_i + m_j + s_{ij}}\right] = 1 \qquad (2.6)$$

To prove the normalization, let us introduce z_{ij} as the sum of m_i and s_{ij} or, in other words, the sum of the population of all the locations in

$$B_{d_{ij}}(i) = \{k \in \mathit{Region}\ A \mid d(i,k) < d_{ij}\}.$$

The series is telescopic and, therefore, its value is easily calculated.

$$m_i \sum_{j \ne i} \left[\frac{1}{z_{ij}} - \frac{1}{z_{ij} + m_j}\right] \overset{\star}{=} m_i \left(\lim_{z_{ij} \to +\infty} \frac{1}{z_{ij}} - \frac{1}{m_i}\right) = 1$$

where in $\star$ is used the following property of the telescopic series.

Proposition 2. *Given the telescopic series*

$$\sum_{k=1}^{+\infty} a_k \quad \text{where} \quad a_k = A_{k+1} - A_k,$$

then, the partial sums s_N consist of

$$s_N = \sum_{k=1}^{N} = A_N - A_0$$

and the value of the series is

$$\sum_{k=1}^{+\infty} a_k = \lim_{N \to +\infty} s_N.$$

Thus, the result in Equation (2.6) is obtained.

Finally, the probability that exactly T_{ij} particles emitted from the origin location i are absorbed in the destination location j is obtained through the marginalization of the probability defined in Equation (2.5): considering

$$\overline{T} = \left\{ T_{ik} \colon k \neq i, j; \sum_{k \neq i} T_{ik} = T_i \right\}$$

the probability is the

$$\begin{aligned} \mathbf{P}(T_{ij} \mid m_i, m_j, s_{ij}) &= \sum_{\overline{T}} \mathbf{P}_i(T_{i1}, T_{i2}, \ldots, T_{ij}, \ldots, T_{iL}) \\ &= \binom{T_i}{T_{ij}} p_{ij}^{T_{ij}} (1 - p_{ij})^{T_i - T_{ij}} \\ &= \frac{T_i!}{T_{ij}!(T_i - T_{ij})!} p_{ij}^{T_{ij}} (1 - p_{ij})^{T_i - T_{ij}} \end{aligned}$$

which is a binomial distribution with average

$$\langle T_{ij} \rangle \equiv T_i p_{ij} = T_i \frac{m_i m_j}{(m_i + s_{ij})(m_i + m_j + s_{ij})}$$

and variance

$$T_i p_{ij} (1 - p_{ij}).$$

Thus, obtaining Equation (2.1).

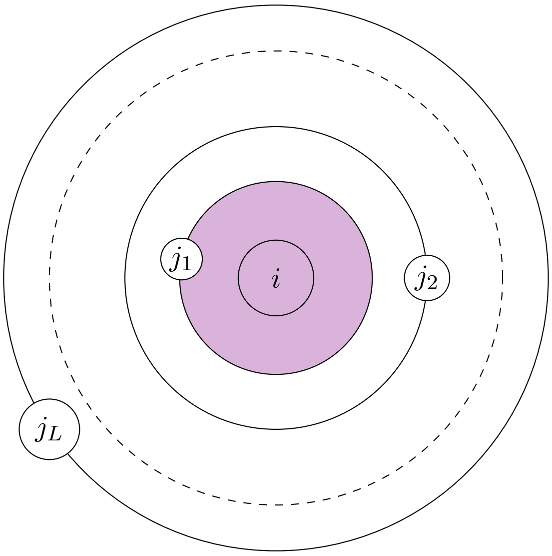

(a) *Initial state of z_{ij} where $d_{ij} = d_{ij_1}$, hence $z_{ij} = m_i$.*

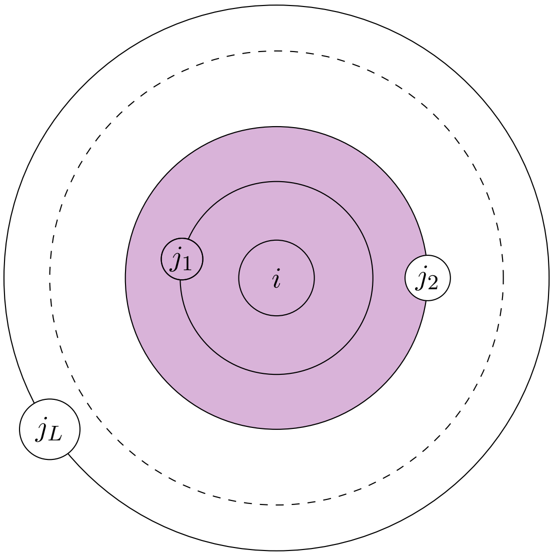

(b) *Second state of z_{ij} where $d_{ij} = d_{ij_2}$, hence $z_{ij} = m_i + m_{j_1}$.*

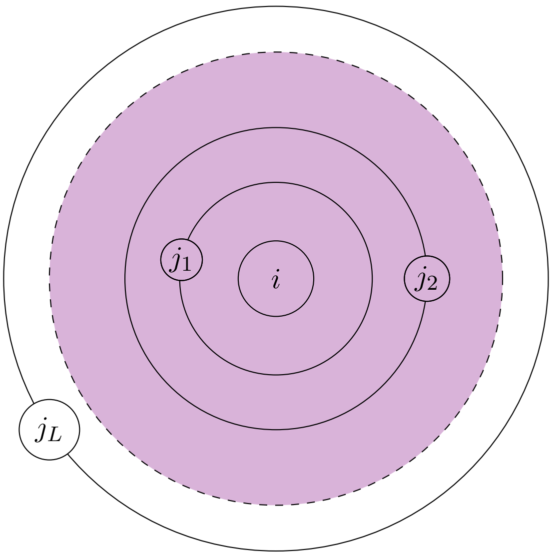

(c) *The process will progressively enlarge d_{ij}.*

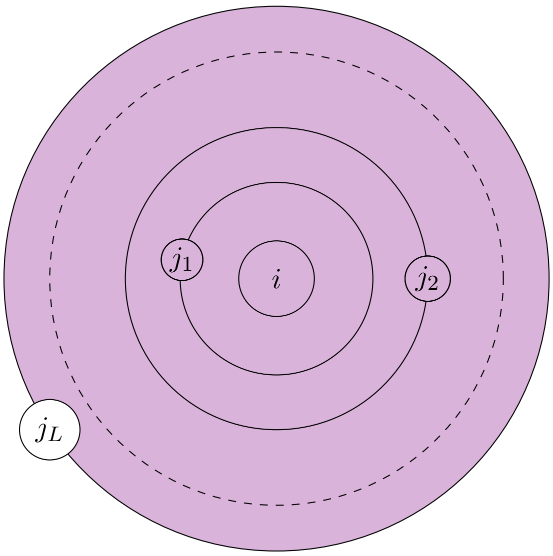

(d) *Last state of z_{ij} where $d_{ij} = d_{ij_L}$, hence $z_{ij} = m_i + \sum_{l=1}^{L} m_{j_l}$.*

Figure 2.3 : *In these Figures, we present an intuitive visualisation of z_{ij}.*

Chapter 3

Comparison between Gravity and Radiation Model

This Chapter will present and compare a visual representation of the results obtained from the gravity and radiation model. After a preliminary presentation of a fictional situation, the Utah example will be retaken into consideration by choosing Davis County as the origin location i and the other counties in this State as the destination locations j (similarly to Section 1.1.3 and Figure 2.2).

3.1 Fictional Case

First and foremost, let us have a clear vision of these models' predictions by concocting a simple yet effective *base case*.

Starting from an $m \times n$ grid, let the cell in position a, b for $1 \leq a \leq m$ and $1 \leq b \leq n$ be the origin location i (also *origin cell*) and all the other cells the destination locations j (also *destination cells*). The cells will be also referred to with $(\cdot, \cdot)$ where $\cdot$ calls for the cell's row and column in the grid.

$$
\begin{array}{c|c|c|c|}
\multicolumn{1}{c}{} & \multicolumn{1}{c}{} & \multicolumn{1}{c}{b} & \multicolumn{1}{c}{} \\
\cline{2-4}
 & j & j & j \\
\cline{2-4}
 & j & j & j \\
\cline{2-4}
a & j & \color{red}{i} & j \\
\cline{2-4}
 & j & j & j \\
\cline{2-4}
\end{array}
$$

Figure 3.1 : *Let it be* $m = 4$, $n = 3$, $a = 3$, $b = 2$.

Now, in order to devise an interesting case which highlights these models, the value s_{ij} has a prominent role. Let us give three distinct *subcases* where s_{ij} determines three different outcomes:

Subcase A: where only in the origin cell and in a single destination cell is the population value positive, otherwise null;

Subcase B: the population has a uniform density throughout the grid, making every cell have the same population value (as used on page 17);

Subcase C: similarly to what happens in reality, there often are agglomerations of people and this behaviour can be implemented by defining a certain cell as the *center* of the agglomeration, with a positive population value, and the adjacent cells (also *periphery cell*) with a lesser positive population value.

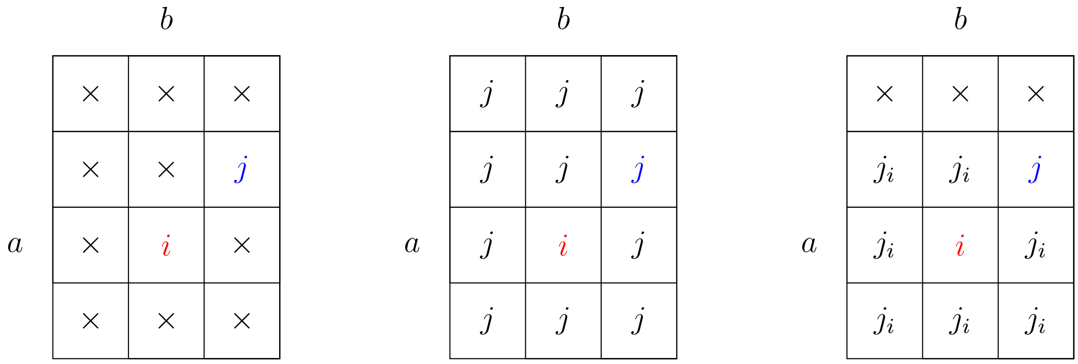

(a) *Subcase A* **(b)** *Subcase B* **(c)** *Subcase C*

Figure 3.2 : *In these Figures, the Subcases above are presented from left to right. The* $\times$ *symbol refers to an empty cell, i.e. a cell with population value null. In Figure 3.2b it is implied* $m_i = m_j$ *hence every cell has the same population value (positive, otherwise this analysis is trivial). In Figure 3.2c,* j_i *refers to the population value around the origin cell that, for easier visualisation, is assumed to decrease uniformly.*

Remark 1. We assume the following:

- we use the gravity law defined in Equation (1.11) and the parameters defined in Table 1.2b from Section 1.1.3;
- the population value is always non-negative and null outside of the grid.

Let us start with *Subcase A*. Supposing *origin cell* in (3,2) and *destination cell* in (2,3) and giving population values

$$m_k = \begin{cases} 100 & \text{if } k = i = \textit{origin cell} \\ 10 & \text{if } k = j = \textit{destination cell} \\ 0 & \text{otherwise} \end{cases}.$$

If we now apply the GM, only the *destination cell* will give a positive value since all the other *non-origin cells* have population value null; the same reason will be obtained with the RM. It is indeed useless to use the RM, reason being

$$T_{ij}\Big|_A^{RM} = T_i \frac{m_i m_j}{(m_i + s_{ij})(m_i + m_j + s_{ij})}\Bigg|_A = T_i \frac{m_i m_j}{m_i m_j} = T_i$$

where we recall T_i being the total amount of commuters departing from i which, having no other destination for the job selection process, will converge in j. Let us stress that the RM *forte* is the ability to use the surrounding population values to increase the precision and prediction power of the model, thus it is not interesting to use it for such a Subcase.

Proceeding with *Subcase B*, let us change from the previous one only the population values as $m_k = 10, \forall k$. Using these simple data, the GM's prediction is readily obtained and it states that the commuter flow will uniformly decrease with the distance. There still is little use in applying the RM because there won't be any improvements if the population is uniformly distributed (refer to page 17).

Lastly, *Subcase C* is the closest to reality among these three. It emulates a simple example of a city, where there is a highly populated area (main districts) surrounded by some lesser populated areas (outskirts). The population values used are

$$m_k = \begin{cases} 100 & \text{if } k = i = \textit{origin cell} \\ 10 & \text{if } k = j = \textit{destination cell} \\ 5 & \text{if } k = j_i = \textit{periphery cell} \\ 0 & \text{otherwise} \end{cases} .$$

In this Subcase, the RM's prediction differs from the GM's: with a non-zero population value, different from the origin one, the value s_{ij} plays a role. It is, yet, not very visible because these Subcases were all simple. Their purpose was to introduce the next Section, where a real scenario will be taken into consideration.

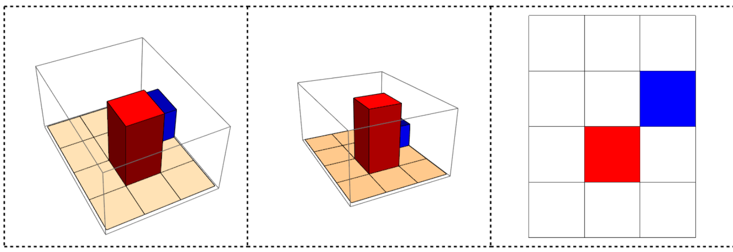

Figure 3.3 : *From left to right: we show the population values in logarithmic scale, the GM values which have little relevance in this Subcase and their 2D-view. The red column (3D) and cell (2D) represent the origin cell i, whereas the blue ones represent the destination cell j.*

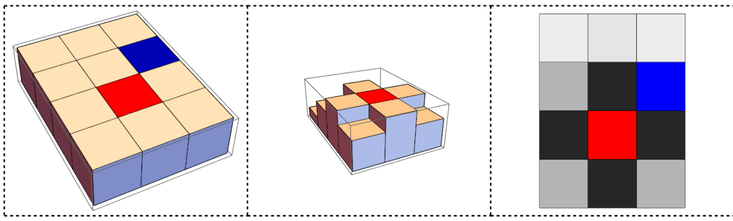

Figure 3.4 : *In this Subcase, these Figures produce a more interesting effect. In the rightmost Figure, we present the expected GM prediction using shades of black where the darker the shade of a cell, the higher the number of commuters arriving at that cell from the origin location.*

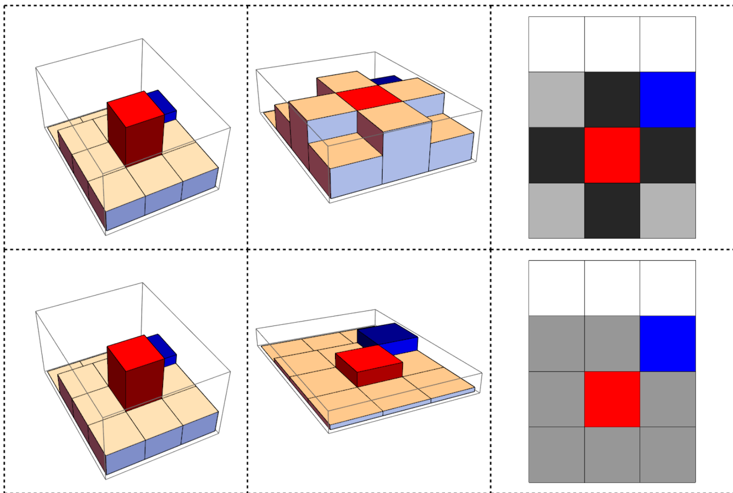

Figure 3.5 : *We present two rows of Figures, each showing the GM and RM's prediction respectively.*

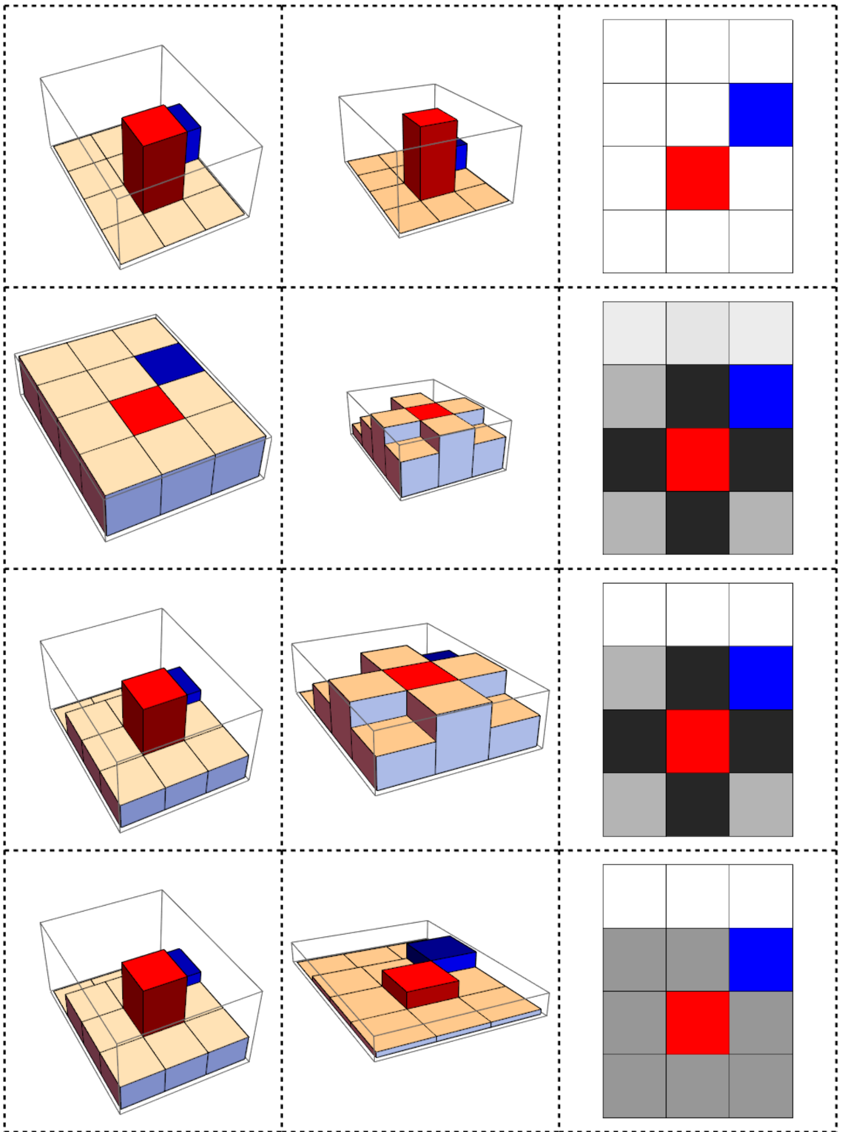

Figure 3.6 : *The results of this Section are here collected for clarity and ease of comparison (from top to bottom: Subcase A with GM, Subcase B with GM, Subcase C with GM and Subcase C with RM)*

3.2 Real Case: Utah

Let us now consider the real-life application of this model that has been used throughout this dissertation. We begin by noting that Utah's Counties' subdivision is already easy to use for this visualisation, however, we will further adjust it to obtain a more practical grid.

	1	2	3	4	5
1	Box Elder N	Cache	Rich	-	-
2	Box Elder S	Weber W	Weber E	-	-
3	Tooele N	Davis	Morgan	Summit	Dagget
4	Tooele C	Salt Lake	Wasatch	Duchesne N	Uintah N
5	Tooele S	Utah W	Utah E	Duchesne S	Uintah C
6	Juab W	Juab E	Sanpete N	Carbon	Uintah S
7	Millard N	Sanpete SW	Sanpete SE	Emery N	Grand N
8	Millard S	Sevier W	Sevier E	Emery S	Grand S
9	Beaver	Piute	Wayne W	Wayne E	San Juan N
10	Iron	Garfield W	Garfield C	Garfield E	San Juan C
11	Washington	Kane W	Kane E	San Juan SW	San Juan SE

Table 3.1 : *Starting from the Counties' subdivision, some adjustments are presented above to obtain a perfect* 11×5 *grid.*

Henceforth, a uniform population distribution inside each County is assumed, unburdening the attribution of this value: data from the U.S. 2012 Census has been used and allocated in accordance with a, sometimes approximate, proportion of each Counties territory inside of each cell (the letters at the end of each name represent approximately which portion of that County has been allocated to that particular cell following the cardinal points).

It is clear that this procedure cannot maintain a perfect correspondence with the real case, but still offers an opportunity to visualise the models' prediction.

	1	2	3	4	5
1	1/3	1	1	-	-
2	2/3	1/2	1/2	-	-
3	1/3	1	1	1	1
4	1/3	1	1	1/2	1/3
5	1/3	1/2	1/2	1/2	1/3
6	2/3	1/3	1/3	1	1/3
7	1/2	1/3	1/3	1/2	1/2
8	1/2	1/2	1/2	1/2	1/2
9	1	1	1/3	2/3	1/3
10	1	1/3	1/3	1/3	1/3
11	1	1/2	1/2	1/6	1/6

Table 3.2 : *An approximate proportion of the Counties mentioned in Table 3.1 will be now used to produce the following.*

	1	2	3	4	5
1	17,145	117,638	2,311	-	-
2	34,290	119,260	119,260	-	-
3	20,030	316,737	10,032	37,593	1,105
4	20,030	1,059,323	24,843	9,768	11,376
5	20,030	267,700	267,700	9,768	11,376
6	7,138	3,568	9,533	22,106	11,376
7	6,430	9,533	9,533	5,634	4,682
8	6,430	10,655	10,655	5,634	4,682
9	6,655	1,591	971	1,941	5,139
10	48,418	1,765	1,765	1,765	5,139
11	142,123	3,744	3,744	2,569	2,569

Table 3.3 : *Combining the information from Table 3.1 and Table 3.2 this Table shows the population value of each cell.*

Using *Subcase C* as inspiration, we apply the same procedure here, with the difference that the population outside of our grid is not null. After noting that the population in a certain range outside of Utah does not present excessive differences in the density amount, we may assume a uniform density to ease the computational phase. With a non-zero population amount, the effect of s_{ij} will highly affect the RM's prediction.

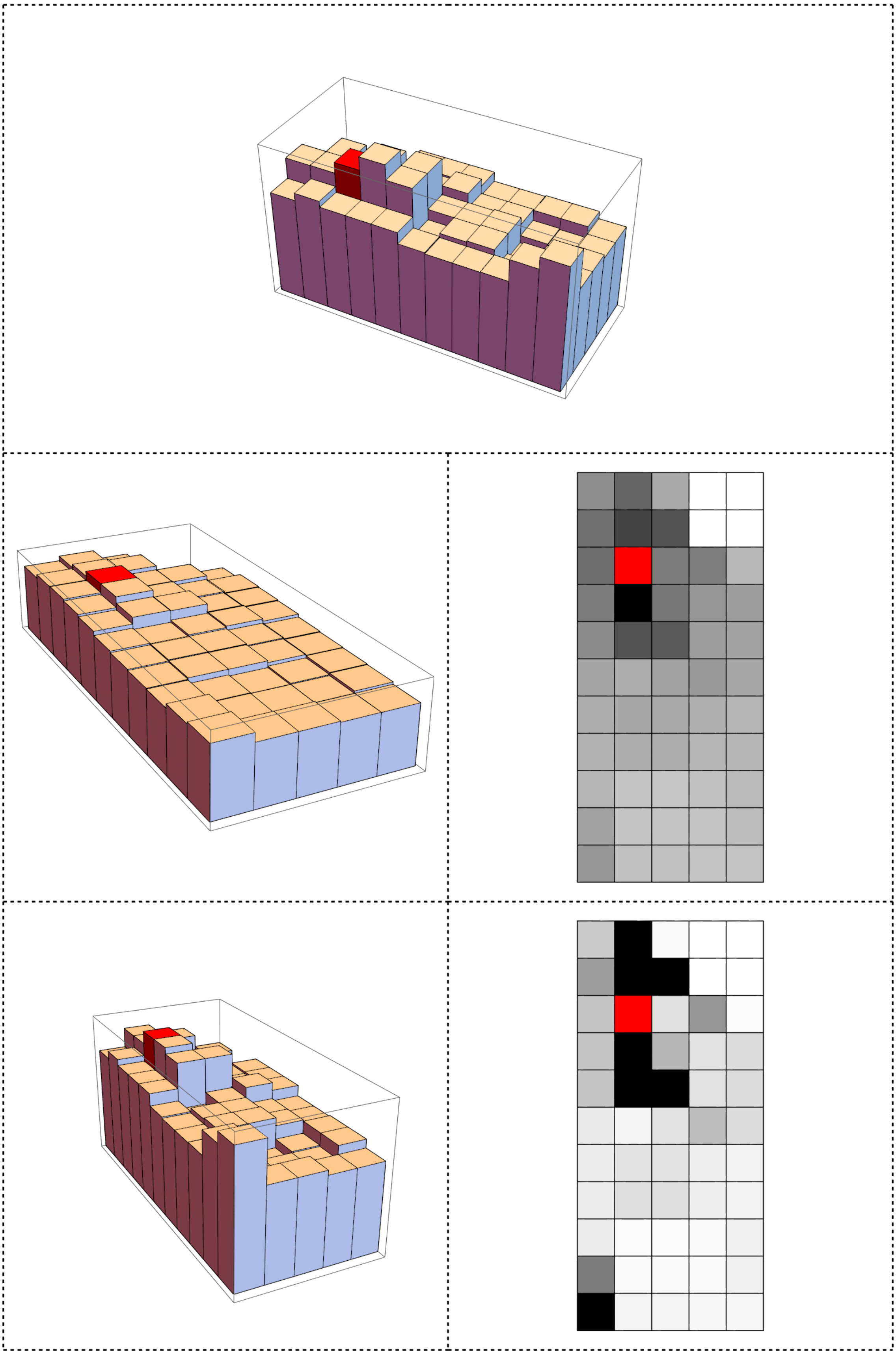

Figure 3.7 : *From top to bottom: we show the population values in logarithmic scale, the GM and RM's prediction.*

Conclusions

The problem of searching for a mathematical underlying model for human mobility patterns and their impacts, e.g. spread of diseases and propagation of information, has lasted decades if not centuries. The Gravity Model monopolised the researchers' attention until some inconsistencies of this model made them question its actual validity.

Focusing on the case of commuters between two locations, we presented this model because it remains a pillar of this branch of science, making its study and comprehension still useful to those who want a deeper knowledge of this theme. Indeed, with intuitiveness as its *forte*, many still hope to adjust its law without having to consider different models [4].

As for us, there were many clear obstacles and inconsistencies which lead us astray from a further optimisation of it. In particular, the necessity of fitting context-specific tunable parameters underlined the limitations of this model, at least in searching for a universal model to predict mobility patterns. Most of these difficulties were overcome by the parameter-free Radiation Model [3] which we subsequently presented. Even though its law is not as simple as the Gravity model, which only considers the masses (e.g. population value) in two locations and their distances, it still is easy to implement.

This new model's core is looking at what determines human mobility, which often is job selection. Taking this into consideration, what ultimately differs the radiation law from the gravity law is the use of the total mass value around the location from which the movement begins up until the distances between the origin and destination location. In other words, the RM's prediction highly differs if the commuter starts its journey from a widely or sparsely populated area.

Nevertheless, this recent take on the modelisation of human patterns should not be taken as the definitive answer. There already are some more generalised forms [9] and new models which aim to surpass it.

As an example, recent studies have shown another intuitive and parameter-free model adapted from Ohm's law of electricity, called the Impedance Model, which provides even more accurate estimations of human mobility, especially when the population distribution is highly heterogeneous [10].

Lastly, we presented some short computational results, which aimed to solidify their differences, both in a fictional and in a real case scenario.

Ringraziamenti

A conclusione di questo elaborato, desidero menzionare alcune delle persone che mi hanno accompagnato in questo importante percorso.

Ringrazio il mio relatore, che in questi mesi mi ha guidato nelle ricerche e nella stesura di questo elaborato, rispondendo sempre celere ai miei dubbi.

Ringrazio di cuore i miei genitori e i parenti tutti. Grazie per avermi sempre sostenuto e per avermi permesso di portare a termine gli studi universitari. Grazie mamma e grazie papà.

Un ringraziamento particolare va ai miei cari colleghi, coi quali ho legato in questi anni. Grazie a voi che avete condiviso con me ansie e soddisfazioni, rendendo nessun giorno ripetitivo e grigio ma sempre descritto da interessanti novità e plurime partite a briscola.

Ringrazio poi, coloro che sono stati sempre a me vicini, dai professori alle amicizie interne e esterne all'università.

È stato un viaggio impegnativo, sia per l'università che per le varie dinamiche della vita. Un viaggio che sono riuscito a superare grazie soprattutto ad alcune persone in particolare. Grazie Costanza, Alberto, Gioele e Filippo.

Infine, vorrei dedicare questo piccolo traguardo a me stesso, che possa essere non la fine, bensì l'inizio di un nuovo ricco percorso.

Appendix

In this Appendix, the *Mathematica* codes used in Chapter 3 are collected.

Some useful functions are:

- `GM` gives the law defining the Gravity Model;
- `RM` gives the law defining the Radiation Model;
- `cuboid` creates a *Graphic3D* structure;
- `FFind` eases to find a cell when the grid is flattened.

```
GM[ci_, cf_] := (ci[[3]]^alpha cf[[3]]^beta)/ Sqrt[(ci[[1]] - cf[[1]])
   ^2 + (ci[[2]] - cf[[2]])^2]^gamma
RM[ci_, cf_, sif_, Ti_] := If[ cf[[3]] == 0, 0, Ti (ci[[3]] cf[[3]])/((
   ci[[3]] + sif) (ci[[3]] + cf[[3]] + sif))]
cuboid[c_] := Cuboid[{c[[1]] - 1, c[[2]] - 1, 0}, {c[[1]], c[[2]], Max
   [0, Log[10, c[[3]] + 0.001]]}]
FFind[i_, j_] := n*(i - 1) + (j - 1) + 1
```

Let us begin with the Fictional Case by introducing the parameters needed.

```
alpha = 0.30;
beta = 0.64;
gamma = 3.05;
m = 4;
n = 3;
ai = 3;
aj = 2;
bi = 2;
bj = 3;
```

For *Subcase A*:

```
grid = Table[{i, j, 0}, {i, 1, m}, {j, 1, n}];
am = 100;
bm = 10;
grid[[ai]][[aj]][[3]] = am;
grid[[bi]][[bj]][[3]] = bm;

a = Map[cuboid, Flatten[grid, 1]];
a[[FFind[ai, aj]]] = {Red, cuboid[grid[[ai]][[aj]]], White};
a[[FFind[bi, bj]]] = {Blue, cuboid[grid[[bi]][[bj]]], White};
aa = Flatten[a, 1];

SUBA = Graphics3D[aa, Ticks -> {Range[11], Range[5], Automatic},
   ViewPoint -> {2, -1, 2}];
(* Export["subA.png",SUBA]*)
```

```
b = Map[GM[grid[[ai]][[aj]], #] &, Drop[Flatten[grid, 1], {FFind[ai, aj
   ]}]];
b1 = Insert[b, am, FFind[ai, aj]];
bb = Partition[b1, n];
gridGM = Table[{i, j, bb[[i]][[j]]}, {i, 1, m}, {j, 1, n}];
maxGM = Max[b];

c = Map[cuboid, Flatten[gridGM, 1]];
c[[FFind[ai, aj]]] = {Red, cuboid[gridGM[[ai]][[aj]]], White};
c[[FFind[bi, bj]]] = {Blue, cuboid[gridGM[[bi]][[bj]]], White};
cc = Flatten[c, 1];
gmSUBA = Graphics3D[cc, Ticks -> {Range[11], Range[5], Automatic},
   ViewPoint -> {2, -1, 1}];
(*Export ["bgmsubA.png",gmSUBA]*)

cub[c_] := {Opacity[(c[[3]])/maxGM, Black], Cuboid[{c[[2]] - 1, -c[[1]]
    + 1}, {c[[2]], -c[[1]]}]}
rectedge[c_] := {EdgeForm[Thickness[Medium]], Transparent, Rectangle[{c
   [[2]] - 1, -c[[1]] + 1}, {c[[2]], -c[[1]]}]};
d = Map[cub, Flatten[gridGM, 1]];
d1 = Map[rectedge, Flatten[gridGM, 1]];
d[[FFind[ai, aj]]] = {Opacity[1, Red], Last[cub[gridGM[[ai]][[aj]]]]};
d[[FFind[bi, bj]]] = {Opacity[1, Blue], Last[cub[gridGM[[bi]][[bj]]]]};
dd = Flatten[d, 1];
dFIN = Join[dd, d1];
GMSUBA = Graphics[dFIN];
(*Export["GMsubA.png",GMSUBA]*)

LA = {SUBA, gmSUBA, GMSUBA};
GLA = GraphicsGrid[{LA}, ImageSize -> {1000, 1000}, FrameStyle ->
   Directive[Thick, Dashed], Frame -> All];

Export["GLA.png", GLA]
```

For *Subcase B*:

```
mB = 10;
grid = Table[{i, j, mB}, {i, 1, m}, {j, 1, n}];
am = mB;
bm = mB;

a = Map[cuboid, Flatten[grid, 1]];
a[[FFind[ai, aj]]] = {Red, cuboid[grid[[ai]][[aj]]], White};
a[[FFind[bi, bj]]] = {Blue, cuboid[grid[[bi]][[bj]]], White};
aa = Flatten[a, 1];

SUBB = Graphics3D[aa, Ticks -> {Range[11], Range[5], Automatic},
   ViewPoint -> {2, -1, 2}];
(* Export["subB.png",SUBB]*)

b = Map[3*GM[grid[[ai]][[aj]], #] &, Drop[Flatten[grid, 1], {FFind[ai,
   aj]}]];
maxGM = Max[b];
b1 = Insert[b, maxGM, FFind[ai, aj]];
bb = Partition[b1, n];
gridGM = Table[{i, j, bb[[i]][[j]]}, {i, 1, m}, {j, 1, n}];
```

```
c = Map[cuboid, Flatten[gridGM, 1]];
c[[FFind[ai, aj]]] = {Red, cuboid[gridGM[[ai]][[aj]]], White};
c[[FFind[bi, bj]]] = {Blue, cuboid[gridGM[[bi]][[bj]]], White};
cc = Flatten[c, 1];
gmSUBB = Graphics3D[cc, Ticks -> {Range[11], Range[5], Automatic},
   ViewPoint -> {2, -1, 1}];
(*Export ["bgmsubA.png",gmSUBA]*)

cub[c_] := {Opacity[(c[[3]]*0.85)/maxGM, Black], Cuboid[{c[[2]] - 1, -c
   [[1]] + 1}, {c[[2]], -c[[1]]}]}
rectedge[c_] := {EdgeForm[Thickness[Medium]], Transparent, Rectangle[{c
   [[2]] - 1, -c[[1]] + 1}, {c[[2]], -c[[1]]}]};
d = Map[cub, Flatten[gridGM, 1]];
d1 = Map[rectedge, Flatten[gridGM, 1]];
d[[FFind[ai, aj]]] = {Opacity[1, Red], Last[cub[gridGM[[ai]][[aj]]]]};
d[[FFind[bi, bj]]] = {Opacity[1, Blue], Last[cub[gridGM[[bi]][[bj]]]]};
dd = Flatten[d, 1];
dFIN = Join[dd, d1];
GMSUBB = Graphics[dFIN];

(*Export["GMsubA.png",GMSUBA]*)

LB = {SUBB, gmSUBB, GMSUBB};
GLB = GraphicsGrid[{LB}, ImageSize -> {1000, 1000}, FrameStyle ->
   Directive[Thick, Dashed], Frame -> All];
Export["GLB.png", GLB]
```

For *Subcase C*:

```
grid = Table[{i, j, 0}, {i, 1, m}, {j, 1, n}];
am = 100;
bm = 10;
grid[[ai]][[aj]][[3]] = am;
grid[[bi]][[bj]][[3]] = bm;

di = Min[m - ai, Abs[ai - bi]];
dj = Min[n - aj, Abs[aj - bj]];
Cond[x_] := If[And[And[Abs[x[[1]] - ai] <= di, Abs[x[[2]] - aj] <= dj],
    Nor[And[x[[1]] == ai, x[[2]] == aj], And[x[[1]] == bi, x[[2]] ==
   bj]]], xtemp = x; xtemp[[3]] = 5; xtemp, xtemp = x; xtemp[[3]] = 0;
    xtemp];
Tsif = Map[Cond, Flatten[grid, 1]];
TTsif = Partition[Tsif, n];

a = Map[cuboid, Flatten[TTsif, 1]];
a[[FFind[ai, aj]]] = {Red, cuboid[{TTsif[[ai]][[aj]][[1]], TTsif[[ai
   ]][[aj]][[2]], am}], White};
a[[FFind[bi, bj]]] = {Blue, cuboid[{TTsif[[bi]][[bj]][[1]], TTsif[[bi
   ]][[bj]][[2]], bm}], White};
aa = Flatten[a, 1];

SUBC = Graphics3D[aa, Ticks -> {Range[11], Range[5], Automatic},
   ViewPoint -> {2, -1, 2}];
(* Export["subC.png",SUBC]*)

grid2 = TTsif;
grid2[[ai]][[aj]][[3]] = am;
grid2[[bi]][[bj]][[3]] = bm;
```

```
b = Map[GM[grid2[[ai]][[aj]], #] &, Drop[Flatten[grid2, 1], {FFind[ai,
    aj]}]];
maxGM = Max[b];
b1 = Insert[b, maxGM, FFind[ai, aj]];
bb = Partition[b1, n];
gridGM = Table[{i, j, bb[[i]][[j]]}, {i, 1, m}, {j, 1, n}];

c = Map[cuboid, Flatten[gridGM, 1]];
c[[FFind[ai, aj]]] = {Red, cuboid[gridGM[[ai]][[aj]]], White};
c[[FFind[bi, bj]]] = {Blue, cuboid[gridGM[[bi]][[bj]]], White};
cc = Flatten[c, 1];
gmSUBC = Graphics3D[cc, Ticks -> {Range[11], Range[5], Automatic},
    ViewPoint -> {2, -1, 1}];
(*Export ["bgmsubC.png",gmSUBC]*)

cub[c_] := {Opacity[(c[[3]]*0.85)/maxGM, Black], Cuboid[{c[[2]] - 1, -c
    [[1]] + 1}, {c[[2]], -c[[1]]}]}
rectedge[c_] := {EdgeForm[Thickness[Medium]], Transparent, Rectangle[{c
    [[2]] - 1, -c[[1]] + 1}, {c[[2]], -c[[1]]}]};
d = Map[cub, Flatten[gridGM, 1]];
d1 = Map[rectedge, Flatten[gridGM, 1]];
d[[FFind[ai, aj]]] = {Opacity[1, Red], Last[cub[gridGM[[ai]][[aj]]]]};
d[[FFind[bi, bj]]] = {Opacity[1, Blue], Last[cub[gridGM[[bi]][[bj]]]]};
dd = Flatten[d, 1];
dFIN = Join[dd, d1];
GMSUBC = Graphics[dFIN];
(*Export["GMsubC.png",GMSUBC]*)

LC = {SUBC, gmSUBC, GMSUBC};
GLC = GraphicsRow[LC, Frame -> All];
(*Export["GLC.png",GLC]*)

T1sif = Tsif;
T1sif[[FFind[ai, aj]]][[3]] = am;
T1sif[[FFind[bi, bj]]][[3]] = bm;
TT1sif = Partition[T1sif, n];
mlist = Table[T1sif[[i]][[3]], {i, 1, Length[Tsif]}];
mT = Total@mlist;
sifP[ai_, aj_, bi_, bj_] := mT - mlist[[FFind[ai, aj]]] - mlist[[FFind[
    bi, bj]]]
Ti = mlist[[FFind[ai, aj]]]/2.0;

b = Map[RM[TT1sif[[ai]][[aj]], #, sifP[ai, aj, #[[1]], #[[2]]], Ti] &,
    Drop[T1sif, {FFind[ai, aj]}]];
maxRM = Max[b];
b1 = Insert[b, maxRM, FFind[ai, aj]];
bb = Partition[b1, n];
gridRM = Table[{i, j, bb[[i]][[j]]}, {i, 1, m}, {j, 1, n}];

c = Map[cuboid, Flatten[gridRM, 1]];
c[[FFind[ai, aj]]] = {Red, cuboid[gridRM[[ai]][[aj]]], White};
c[[FFind[bi, bj]]] = {Blue, cuboid[gridRM[[bi]][[bj]]], White};
cc = Flatten[c, 1];
rmSUBC = Graphics3D[cc, Ticks -> {Range[11], Range[5], Automatic},
    ViewPoint -> {2, -1, 1}];
(*Export ["brmsubC.png",rmSUBC]*)

cub[c_] := {Opacity[(c[[3]]*0.85)/maxRM, Black], Cuboid[{c[[2]] - 1, -c
```

```
   [[1]] + 1}, {c[[2]], -c[[1]]}]}
rectedge[c_] := {EdgeForm[Thickness[Medium]], Transparent, Rectangle[{c
   [[2]] - 1, -c[[1]] + 1}, {c[[2]], -c[[1]]}]};
d = Map[cub, Flatten[gridRM, 1]];
d1 = Map[rectedge, Flatten[gridRM, 1]];
d[[FFind[ai, aj]]] = {Opacity[1, Red], Last[cub[gridRM[[ai]][[aj]]]]};
d[[FFind[bi, bj]]] = {Opacity[1, Blue], Last[cub[gridRM[[bi]][[bj]]]]};
dd = Flatten[d, 1];
dFIN = Join[dd, d1];
RMSUBC = Graphics[dFIN];
(*Export["RMsubC.png",RMSUBC]*)

LC1 = {SUBC, rmSUBC, RMSUBC};
GLC1 = GraphicsRow[LC1, Frame -> All];
(*Export["GLC1.png",GLC1]*)

GLCT = GraphicsGrid[{LC, LC1}, ImageSize -> {1000, 1000}, FrameStyle ->
    Directive[Thick, Dashed], Frame -> All];
Export["GLCT.png", GLCT]

GLT = GraphicsGrid[{LA, LB, LC, LC1}, ImageSize -> {1000, 1000},
   FrameStyle -> Directive[Thick, Dashed], Frame -> All]
Export["GLT.png", GLT]
```

Let us comment on some functions and parameters:

- `cub` and `rectedge` give a *Graphics* structure;
- `Cond` helps us increment the population values around the origin location;
- `sifP` gives a *pseudo*-value of s_{ij}, it suffices this form since in this Subcase the problem is significantly simplified;
- `Ti` is the value T_i of the Radiation Model.

Finally, the Real-life Case.

```
alpha = 0.24;
beta = 0.14;
gamma = 0.29;
PopCellUtah = {{17145, 117638, 2311, 0, 0}, { 34290, 119260, 119260, 0,
    0}, {20030, 316737, 10032, 37593, 1105}, {20030, 1059323, 24843,
   9768, 11376 }, { 20030, 267700, 267700, 9768, 11376 }, { 7138,
   3568, 9533, 22106, 11376 }, { 6430, 9533, 9533, 5634, 4682}, {6430,
    10655, 10655, 5634, 4682}, {6655, 1591, 971, 1941, 5139}, {48418,
   1765, 1765, 1765, 5139}, {142123, 3744, 3744, 2569, 2569}};
m = 11;
n = 5;
ai = 3;
aj = 2;
TTsif = Table[{i, j, PopCellUtah[[i]][[j]]}, {i, 1, m}, {j, 1, n}];
Tsif = Flatten[TTsif, 1];

a = Map[cuboid, Tsif];
a[[FFind[ai, aj]]] = {Red, cuboid[TTsif[[ai]][[aj]]], White};
aa = Flatten[a, 1];
UT = Graphics3D[aa, Ticks -> {Range[11], Range[5], Automatic},
   ImageSize -> {2000, 1000}];
(* Export["UT.png",UT]*)
```

```
di = Min[m - ai, ai, Abs[ai - bi]];
dj = Min[n - aj, aj, Abs[aj - bj]];
grid2 = TTsif;
b = Map[GM[grid2[[ai]][[aj]], #] &, Drop[Flatten[grid2, 1], {FFind[ai,
    aj]}]];
maxGM = Max[b];
b1 = Insert[b, maxGM, FFind[ai, aj]];
bb = Partition[b1, n];
gridGM = Table[{i, j, bb[[i]][[j]]}, {i, 1, m}, {j, 1, n}];

c = Map[cuboid, Flatten[gridGM, 1]];
c[[FFind[ai, aj]]] = {Red, cuboid[gridGM[[ai]][[aj]]], White};
cc = Flatten[c, 1];
gmUT = Graphics3D[cc, Ticks -> {Range[11], Range[5], Automatic},
    ImageSize -> {1000, 1000}, ViewPoint -> {2, -1, 1}];
(*Export ["bgmUT.png",gmUT]*)

cub[c_] := {Opacity[(c[[3]])/maxGM, Black], Cuboid[{c[[2]] - 1, -c[[1]]
     + 1}, {c[[2]], -c[[1]]}]}
rectedge[c_] := {EdgeForm[Thickness[Medium]], Transparent, Rectangle[{c
    [[2]] - 1, -c[[1]] + 1}, {c[[2]], -c[[1]]}]};
d = Map[cub, Flatten[gridGM, 1]];
d1 = Map[rectedge, Flatten[gridGM, 1]];
d[[FFind[ai, aj]]] = {Opacity[1, Red], Last[cub[gridGM[[ai]][[aj]]]]};
dd = Flatten[d, 1];
dFIN = Join[dd, d1];
GMUT = Graphics[dFIN, ImageSize -> {1000, 1000}];
(*Export["GMUT.png",GMUT]*)

LGUT = {UT, gmUT, GMUT};
GGLUT = GraphicsRow[LGUT, Frame -> All];
(*Export["GGLUT.png",GGLUT]*)

Utahsize = 219887;
NEcell = 11.0*5 - 4;
cellsize = Utahsize/NEcell;
Wyomingsize = 253596;
Wyomingpop = 580803;
WNcell = Wyomingsize/cellsize;
AVcellpop = Wyomingpop/WNcell;

ddi[bi_] := Min[m - ai, ai, Abs[ai - bi]];
ddj[bj_] := Min[n - aj, aj, Abs[aj - bj]];
InsideUT[x_, bi_, bj_] := Abs[x[[1]] - ai] <= ddi[bi] && Abs[x[[2]] -
    aj] <= ddj[bj] && Not[x[[1]] == 0 || x[[2]] == 0]
InsideRange[x_, bi_, bj_] := Abs[x[[1]] - ai] <= Abs[ai - bi] && Abs[x
    [[2]] - aj] <= Abs[aj - bj]
czero = 0;
Countcond[x_, bi_, bj_, czero_] := If[InsideRange[x, bi, bj], If[
    InsideUT[x, bi, bj], cz = czero; cz += PopCellUtah[[x[[1]]]][[x
    [[2]]]]; cz, cz = czero; cz += AVcellpop; cz], cz = czero; cz]

mm = Floor[m*1.5];
nn = Floor[n*1.5];
mTotP = Table[Total@Map[Countcond[#, i, j, 0] &, Flatten[Table[{k, l},
    {k, -mm, mm}, {l, -nn, nn}], 1]], {i, 1, m}, {j, 1, n}];
mTot = Table[mTotP[[i]][[j]] - PopCellUtah[[ai]][[aj]] - PopCellUtah[[i
```

```
    ]][[j]], {i, 1, m}, {j, 1, n}];
mTot[[ai]][[aj]] = 0;
Ti = PopCellUtah[[ai]][[aj]]/2.0;
b = Map[RM[TTsif[[ai]][[aj]], #, mTot[[ai]][[aj]], Ti] &, Drop[Tsif, {
    FFind[ai, aj]}]];
maxRM = Max[b];
b1 = Insert[b, maxRM, FFind[ai, aj]];
bb = Partition[b1, n];
gridRM = Table[{i, j, bb[[i]][[j]]}, {i, 1, m}, {j, 1, n}];

c = Map[cuboid, Flatten[gridRM, 1]];
c[[FFind[ai, aj]]] = {Red, cuboid[gridRM[[ai]][[aj]]], White};
cc = Flatten[c, 1];
rmUT = Graphics3D[cc, Ticks -> {Range[11], Range[5], Automatic},
    ImageSize -> {1000, 1000} , ViewPoint -> {2, -1, 1}];
(*Export ["brmUT.png",rmUT]*)

cub[c_] := {Opacity[(c[[3]]*3)/maxRM, Black], Cuboid[{c[[2]] - 1, -c
    [[1]] + 1}, {c[[2]], -c[[1]]}]}
rectedge[c_] := {EdgeForm[Thickness[Medium]], Transparent, Rectangle[{c
    [[2]] - 1, -c[[1]] + 1}, {c[[2]], -c[[1]]}]};
d = Map[cub, Flatten[gridRM, 1]];
d1 = Map[rectedge, Flatten[gridRM, 1]];
d[[FFind[ai, aj]]] = {Opacity[1, Red], Last[cub[gridRM[[ai]][[aj]]]]};
dd = Flatten[d, 1];
dFIN = Join[dd, d1];
RMUT = Graphics[dFIN, ImageSize -> {1000, 1000}];
(*Export["RMUT.png",RMUT]*)

LRUT = {UT, rmUT, RMUT};
GRLUT = GraphicsRow[LRUT, Frame -> All];
(*Export["GLUT.png",GLUT]*)

FGLUT = GraphicsGrid[{{UT, SpanFromLeft}, {gmUT, GMUT}, {rmUT, RMUT}},
    FrameStyle -> Directive[Thick, Dashed], Frame -> All];
FFGLUT = Show[FGLUT, ImageSize -> Full];
Export["FGLUT.png", FFGLUT]
```

Let us comment on some functions and parameters:

- `alpha`, `beta` and `gamma` are changed accordingly to Table 1.2b;
- `PopCellUtah` contains the values of Table 3.3;
- `AVcellpop` is the value given to the cells surrounding Utah;
- `InsideUT` checks if a cell is inside the grid;
- `Inside Range` checks if a cell is inside the range of s_{ij}, i.e. d_{ij};
- `CountCond` ultimately gives `mTotP` and then `mTot` which is the collection of s_{ij} for every cell in the grid.

Bibliography

[1] Dirk Brockmann, Lars Hufnagel, and Theo Geisel. The scaling laws of human travel. *Nature*, 439, 2006.

[2] Hank Eskin. Where is George? *https://www.wheresgeorge.com*.

[3] Filippo Simini, Marta González, Amos Maritan, and Albert-László Barabási. A universal model for mobility and migration patterns. *Nature*, 484, 2012.

[4] Alan Deardorff. Determinants of bilateral trade: does gravity work in a neoclassical world? In *The regionalization of the world economy*. University of Chicago Press, 1998.

[5] Alan Geoffrey Wilson. A statistical theory of spatial distribution models. *Transportation Research*, 1, nov 1967.

[6] Alan Geoffrey Wilson. The use of entropy maximising models, in the theory of trip distribution, mode split and route split. *Journal of transport economics and policy*, 1969.

[7] Duygu Balcan, Vittoria Colizza, Bruno Gonçalves, Hao Hu, José J Ramasco, and Alessandro Vespignani. Multiscale mobility networks and the spatial spreading of infectious diseases. *Proceedings of the national academy of sciences*, 106, 2009.

[8] Cécile Viboud, Ottar Bjørnstad, David Smith, Lone Simonsen, Mark Miller, and Bryan Grenfell. Synchrony, waves, and spatial hierarchies in the spread of influenza. *Science*, 312, 2006.

[9] Christian Alis, Erika Fille Legara, and Christopher Monterola. Generalized radiation model for human migration. *Scientific reports*, 2021.

[10] Kankoé Sallah, Roch Giorgi, Linus Bengtsson, Xin Lu, Erik Wetter, Paul Adrien, Stanislas Rebaudet, Renaud Piarroux, and Jean Gaudart. Mathematical models for predicting human mobility in the context of infectious disease spread: introducing the impedance model. *International journal of health geographics*, 16, 2017.